Steel and Composite Structures, *Vol. 22*, *No. 2* (*2016*) *387-398*
DOI: http://dx.doi.org/10.12989/scs.2016.22.2.387

Flexural behavior of UHPC-RC composite beam

Xiangguo Wu [*1,2] and Yang Lin [1,2a]

[1] *Key Lab of Structures Dynamic Behavior and Control of the Ministry of Education*, *Harbin Institute of Technology*, *Harbin*, *150090*, *China*
[2] *School of Civil Engineering*, *Harbin Institute of Technology*, *Harbin*, *150090*, *China*

(*Received January 21*, *2016*, *Revised September 29*, *2016*, *Accepted October 12*, *2016*)

Abstract. In order to evaluate the effects of U shape ultra high performance concrete (UHPC) permanent form on the behaviors of Reinforced Concrete (RC) beam, a full scale RC composite beam is designed and tested with U shape UHPC permanent form and a reference RC beam with same parameters is tested simultaneously for comparison. The effects of the permanent form on the failure mode, cracking strength, ultimate capacity and deformation are studied. Test results shows that the contributions of the U shape UHPC permanent form to the flexural cracking behaviors of RC beam are significant. This study may provide a reference for the design of sustainable RC beam with high durable UHPC permanent form.

Keywords: composite beam; cracking strength; flexural capacity; permanent form; ultra high performance concrete

1. Introduction

Ultra high performance concrete (UHPC) as a new generation of high performance concrete, shows ultra high strength, ductility, and durable properties (Benjamin 2006, Wu *et al*. 2008). A sustainable structure component can be realized by using precast UHPC element as the permanent form of the cast-in-situ reinforced concrete (RC) component, such as beam. Using UHPC permanent form design, not only durable structure design can be realized, but the failure modes, loading capacity of the structural members can also be improved. These improvements can be attributed to the composites effects between precast UHPC unit and cast-in-situ core (RC). In recent years, the similar studies, i.e., existing RC structure rehabilitated by cast-in-situ UHPC layer, illustrated this point, such as Habel (2004), Noshiravani and Bruhwiler (2013), etc. Thin wall precast UHPC element has also been applied in rehabilitation and strengthening of existing structures, such as Bencardino and Condello (2014), Massicotte *et al*. (2013a and b), Mohammed *et al*. (2015).

Different from the existing structures component rehabilitation, precast technique is used in UHPC permanent form and core RC is cast in situ. Some studies in this area are given in Wu *et al*. (2011), Hong and Kang (2013), Wu *et al*. (2013a, b, 2014), Yuan *et al*. (2013, 2014), Wirojjanapirom *et al*. (2013). The shear properties of UHPC composite beam were studied by

*Corresponding author, Professor, E-mail: wuxiangguo@hit.edu.cn
[a] Post-Graduate, E-mail: linyang@163.com

http://www.techno-press.org/?journal=scs&subpage=6 ISSN: 1229-9367 (Print), 1598-6233 (Online)

Wirojjanapirom *et al*. (2013), in which the effects of thickness of UHPC, the contact surface roughness, shear bolts and stirrups on the composite beam mechanical property were investigated.

Due to the high mechanical properties of UHPC, internal stress redistribution will occur between the core RC and UHPC unit in the loading process (Lou *et al*. 2015). Especially due to the size effect of the material tensile properties, precast UHPC element with thinner thickness has more potential for improving the cracking capacity. Recently, related research include UHPC composites column, such as Guler *et al*. (2012, 2013).

The effect of fiber distribution on bearing capacity of UHPC structure is great, especially thin wall UHPC element (Bencardino 2013). Because of the random distribution of fiber, material cracking generally initiates from relatively weak zone. Cracking is disadvantageous for realizing high durable structure design. Wire meshed UHPC is proposed for thin wall precast permanent form in this paper to improve the homogeneity of material anisotropy. In order to investigate the effects of the precast wire meshed UHPC unit on flexural behavior of RC beam, a full scale UHPC-RC composite beam are designed and tested. A reference normal RC beam with the same design parameters, i.e., same section dimension and same reinforcement ratio, is tested simultaneously. The influences of precast UHPC unit on the cracking strength, ultimate bearing capacity, and ductility and failure mode of the new type composite beam are studied. This study shows that the precast wire meshed UHPC unit can be a multi functional permanent form, i.e., the high durable protection layer and effective improvement of the structural behaviors. This study can be a reference for the future study and engineering design of the innovative high durable composites structure.

2. Material properties and specimen design

2.1 Material properties

The quality mixture ratio of UHPC used for the permanent form is shown in Table 1. Cement is 425 ordinary Portland cement. Silica content of silica fume is 85%. The average particle diameter of silica fume is 0.1~0.3 μm and its specific surface area is 20~28 m^2/g. Heavy calcium carbonate powder with particle size 0.04mm is used as filling powder. In order to further optimize the cost of material, quartz sand is replaced by ordinary river sand with apparent density of 2.62 g/cm^3, fineness modulus of 2.6, mud content of 0.2%. High strength copper and stainless steel fiber are used in the UHPC mixing with diameter 0.2 mm and length 13 mm. The tensile strength is 1800 MPa. Polycarboxylate superplasticizer with solid content of 40% is used in the material.

The mixing and steam curing process are same as the general UHPC manufacturing methods which can be referenced from Wu *et al*. (2013a, b, and 2014) and Rizzuti and Bencardino (2014).

The maximum cubic compressive strength with dimension 100 mm is 136.5 MPa, the minimum compressive strength is 119.8 MPa, and average compressive strength is 129.7 MPa. The corresponding standard deviation is 12.4 MPa.

C30 commercial concrete is used in the RC. The maximum compressive strength of normal

Table 1 The mixture ratio of UHPC

Cement	Silica fume	Filling powder	Fine sand	water	Steel fiber	Super plasticizer
1	0.25	0.3	1.1	0.2	0.015	0.036

concrete is 30.3 MPa, the minimum compressive strength is 25.8 MPa, and the average compressive strength is 28.2 MPa. The corresponding standard deviation is 3.2 MPa.

The wire mesh with dimension of mesh 6 mm × 6 mm and wire diameter 0.6 mm is used in this test. The tensile strength of the wire is 300 MPa.

Hot rolled ribbed steel bar with standard yielding strength 400 MPa (HRB400) is used as longitudinal rebar in the beam and the rebar diameter is 18 mm (3C18). Hot rolled plain steel bar with standard yielding strength 300 MPa (HPB300) is used as the stirrup in the beam and stirrup diameter is designed as 8 mm with a constant spacing of 100 mm (A8@100). Three samples were tested for every kind of steel bar. The maximum, minimum and average tensile yielding strength of HRB400 are 408 MPa, 402 MPa, and 405 MPa, respectively. The maximum, minimum and average tensile strength of HRB400 are 460.2 MPa, 420.6 MPa, and 445.4 MPa, respectively. The maximum, minimum and average tensile yielding strength of HPB300 are 306.4 MPa, 304.5 MPa, and 301.8 MPa, respectively. The maximum, minimum and average tensile strength of HPB300 are 346.8 MPa, 322.7 MPa, and 341.5 MPa, respectively. The E-modulus of the rebar of HRB400 and HPB300 are 200 GPa.

Steel bolt made by ordinary carbon steel with standard yielding strength 320 MPa and ultimate tensile strength 400 MPa is used as connector and its diameter is 16 mm.

2.2 Specimen,test setup and instrumentation

The simply supported beams of normal reinforced concrete beam (NCB) and UHPC-RC composite beam (UCB) are designed, in which NCB is the reference specimen. Longitudinal rebar and stirrup in the two beams are the same, and cross section size of the two beams is 200 mm × 400 mm. The length of the beams is 2300 mm with a clear span of 2100 mm. The element thickness of the U shape UHPC is 20 mm. HRB400 bar is used as the longitudinal rebar, HPB300 bar is used as stirrup and top bar. Specifically, 3C18 are in the tensile face (bottom face) and 2A8 are in compression face (top face or upper face) of the beams. The top bar is disconnected to avoid appearing double reinforcement beam in pure bending section of beam. The dimension and reinforcement information of the two beams are shown in Figs. 1(a)-(b), respectively. The nominal diameter of the bolt connector is 16 mm and its longitudinal constant space is 200 mm. The parameters of the two beams are presented in Table 2, in which “A” represents “HPB300” with standard yield strength 300 MPa and “C” represents “HRB400” with yield standard strength 400 MPa.

The wooden forms are used for UHPC element and are removed after casting 24 h. UHPC element are cured with conditions of the temperature of 90 ± 2°C, the humidity of 95%, and steam curing time of 48 h.

Test setup is shown in Fig. 2. The load device was a 100 ton hydraulic servo testing instrument which was arranged in the midpoint of the distribution beam. The distance between the two loading points is 500 mm and pure bending behavior can be investigated from this region. Strain gauges were arranged in the midpoint of the three longitudinal bars. The average value of the three measuring values will be final test value. In shear span, four strain gauges were attached in the diagonal line between the loading point and support as shown in Figs. 1(a) and (b) with number #1~#4. In pure bending region, four strain gauges were attached in the midpoint of the two bolt connectors and the attaching method is same as the rebar strain gauge, i.e., bolt local surface grinding and bonding strain gauge by glue. Additionally, five strain gauges were attached in the mid-span surface of the beam concrete. As shown in Fig. 2, five Linear Variable Displacement

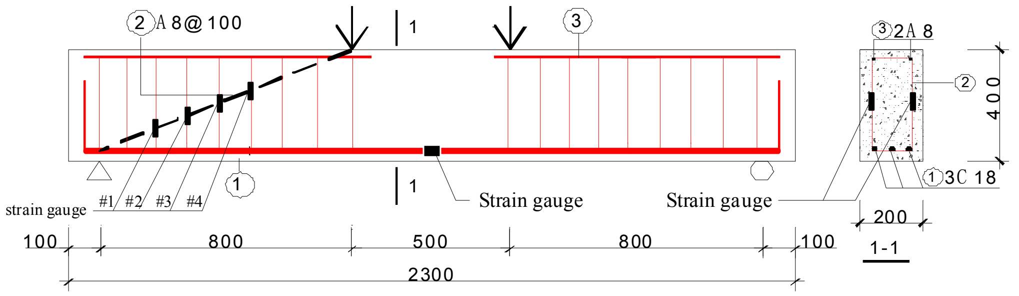

(a) Dimension and reinforcement of NCB

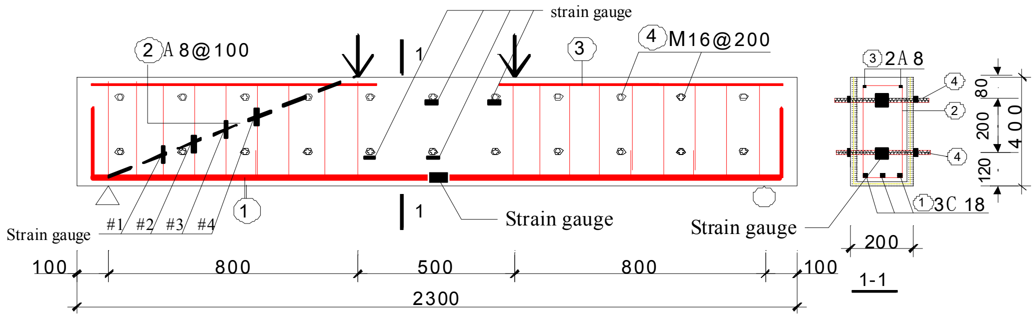

(b) Dimension and reinforcement of UCB

Fig. 1 Cross sections and reinforcement of the two tested beams

Table 2 Basic parameters

Specimen number	Span (m)	Longitudinal rebar		Stirrups
		upper	bottom	
NCB	2.1	2A18	3C18	A8@100
UCB	2.1	2A18	3C18	A8@100

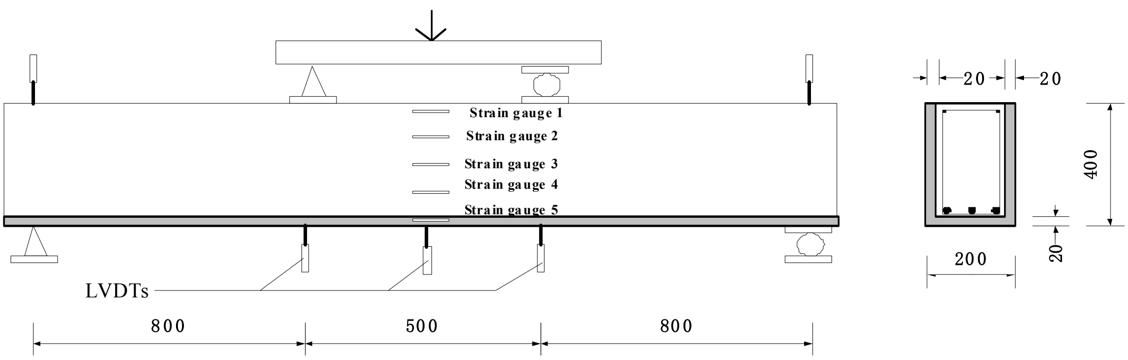

Fig. 2 Composite beam loading instrument

Transducers (LVDTs) were attached to measure the displacement in which three LVDTs were attached in the pure bending region and two LVDTs were attached at the ends of the beam to measure the possible upward displacement due to the bending rotation. The LVDTs is spring type with rail spring. The LVDTs type is SDVH20 with diameter 20 mm and its measuring scope is 0-50 mm.

Two-point loading was statically applied, as shown in Fig. 2. Loading step was 10 kN. There was preload 30 kN before formal loading to confirm the instrument work normally. The load at cracking, yielding and ultimate are recorded, in which cracking load is equal to the first visible crack load, yielding load is equal to the load at yielding of the tension rebar, and the ultimate load is equal to the load at ultimate limit of the beam.

3. Structure behavior and experimental results

3.1 Loading process and structural behavior

3.1.1 structural behavior of NCB

As shown in Fig. 3, NCB specimen was loaded with step 10 kN in the process from start to beam failure. When loading to 48 kN, the first visible crack formed, and located at the bottom of the loading section; there were 5 micro cracks under this load step, and the corresponding displacement was 0.54 mm. The first crack propagated with the increasing of load. There were 6 long cracks that developed in the section over half of the height when load reached 87 kN, and then, cracks propagated and connected. The loading process are shown in Figs. 3(a)~(b) from

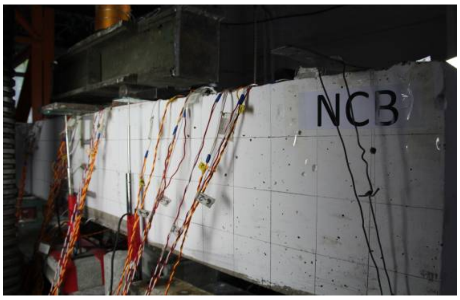

(a) NCB ready for loading

(b) NCB loading beyond cracking load

(c) Crack distribution

(d) Mid-span crack after unloading

Fig. 3 Load and failure status of NCB

ready for loading state, cracking state to the unloading state. Finally, 6 major macro-cracks were formed in pure bending of beam while few new cracks were formed in other location of beam, several major cracks expanded to compressive zone, and the width of crack increased. Significantly, rebar in the tension zone began to yield when load reached to 215 kN, the width of the 5 major cracks in the pure bending section was more than 2 mm, and crack height was increasing, over 3/4 of the height of beam. At this time, the concrete in the compression zone was crushed, and beam reached ultimate state.

The displacement in mid-span was 8.65 mm when beam yield. Load no longer increased while the cross displacement was still increasing. But when the cross displacement was 24.8 mm, the bearing capacity of beam further improved, and the peak load is 304 kN, but the stable ultimate load was 276 kN, at this time, rebar reached at the head of strengthen stage. There were a total of 139 cracks in the process of the NCB's loading to failure. LVDT was removed in the last period of the test for instrument safety.

3.1.2 Structural behavior of UCB

As shown in Fig. 4, the loading method of UCB specimen was the same as NCB specimen. When loading to 102 kN, the first crack occurred at the bottom of the loading section, and there were 4 micro cracks under this level of load which located in pure bending section. When the first crack appeared, displacement in mid-span was 0.97 mm. The first crack did not propagate further, but a new micro crack was appeared in other position. In the loading process, there were a few cracks interconnected, but in pure bending section, a lot of parallel vertical cracks appeared, and crack height was small. The crack whose length was more than the half of the section's height did not appear until 220 kN. With the load continuously increasing, a few cracks were appeared and its

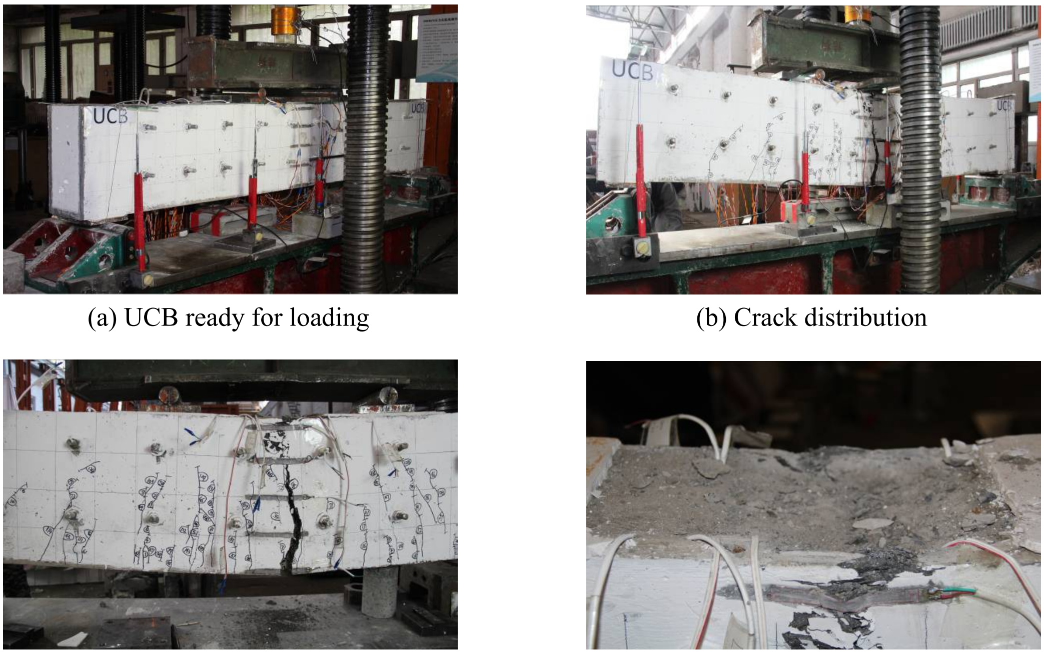

(a) UCB ready for loading
(b) Crack distribution
(c) Major crack at ultimate state
(d) Compression zone at ultimate state

Fig. 4 Loading and destruction status of UCB length was between the half of the section's height and 3/4 of the section's height, and the width of cracks was still small. When the load was increased to 292 kN, the bottom of the UHPC element was broken, and steel fiber was pulled out, the longitudinal rebar in the cracks immediately reached the yield, the crack width rapidly changed bigger, the compression zone decreased rapidly and reached its ultimate compressive strain, then compression zone was collapsed, UCB reached to ultimate bearing capacity. There appeared a total of 151 cracks in the loading process of the UCB, which was more 12 cracks than NCB, and finally the cracks that made beam failure appeared in the mid-span of beam, and there was only one major crack, and the propagation of crack was very slow before the failure state. Crack width increased rapidly when the load reached to the failure load. The loading process of UCB are shown in Figs. 4(a)~(d) from ready for loading state, to crack distribution during loading, and the major crack at ultimate state.

3.2 Test results

The test results of cracking load, cracking displacement, and ultimate load of the two specimens are listed in Table 3. Load-displacement curves of UCB and NCB are shown in Fig. 5.

3.2.1 Load-displacement curve

Loading capacity

It can be seen from the result that the cracking load and ultimate load of UCB is wholly higher than NCB. The ultimate load of UCB is 1.06 times of NCB, and the cracking load of UCB is 2.13 times of NCB. Compared with the ultimate load, the cracking load is improved significantly.

Table 3 Results of tested beams

Specimen	Load (kN)			Displacement (mm)			μ_y
	Cracking	Yielding	Ultimate	Cracking	Yielding	Ultimate	
NCB	48	215	276	0.54	8.65	24.8	2.87
UCB	102	292	292	0.97	5.14	32.6	6.34

Here, μ_y is the deflection ductility index and it is equal to the ratio of ultimate displacement and yielding displacement

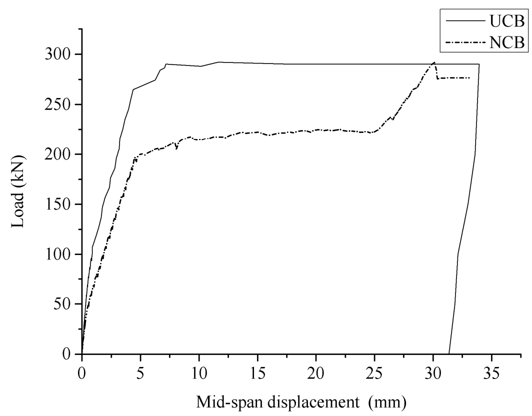

Fig. 5 Load-Displacement curves

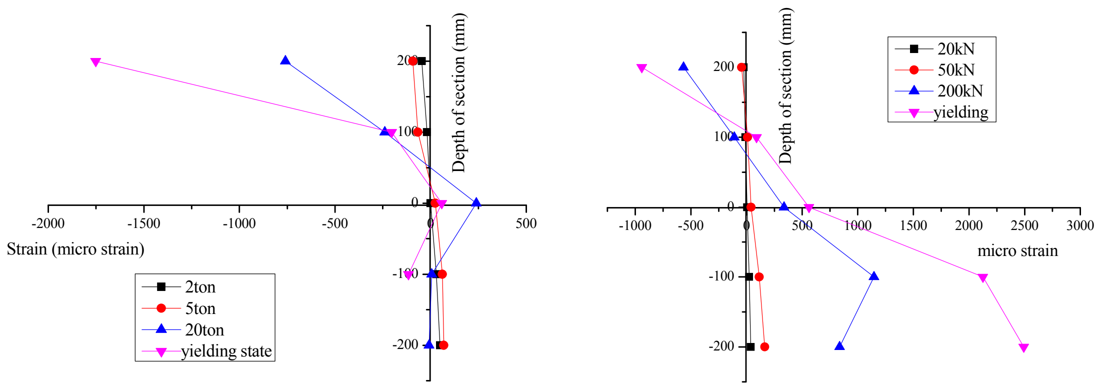

(a) NCB (b) UCB

Fig. 6 Strain of concrete in the cross-section

Stiffness

From the load-displacement curve, the slope of the load-displacement curve of UCB is larger than that of NCB, which indicates that flexural stiffness of composite beam is increased by the precast UHPC element. With the appearance of cracks, steel fiber of precast UHPC element can continuously transfer the principal tensile stress of the vertical direction of the cracks, so the stiffness degradation of UCB is small with crack increasing. This behavior may delay the crack propagation.

3.2.2 Concrete strain

Under different load stages, the strain comparison of concrete in NCB and UCB are shown in Figs. 6(a) and (b).

3.2.3 Longitudinal rebar strain

Strains of the longitudinal rebar of NCB and UCB are shown in Fig. 7. It can be seen that at the same load level the tensile strain of longitudinal rebar in the UCB is less than that in NCB, which

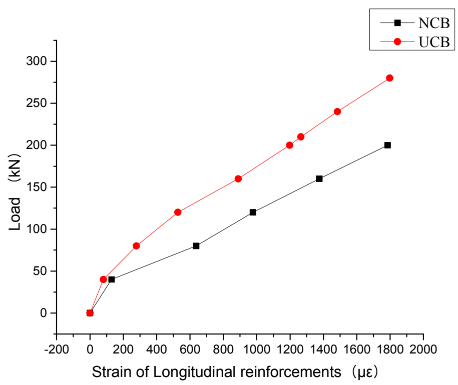

Fig. 7 Comparison of longitudinal rebar strain under different load

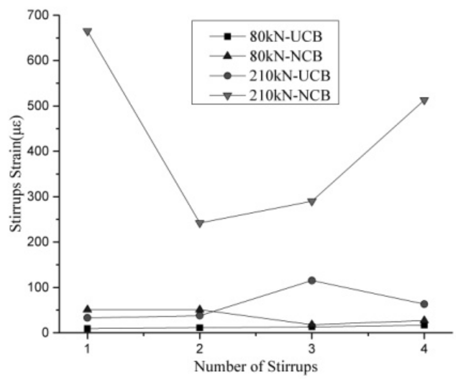

Fig. 8 Comparison of the stirrup strain under the same vertical load

can be attributed to the contribution of precast UHPC element. Under the load of 215 kN, longitudinal rebar in NCB yield, while under the load of 280 kN, the longitudinal rebar strain in UCB is still linear elastic, and the longitudinal rebar is not yield. Thus, for same under reinforcement level design, the reinforcement ratio can be reduced.

3.2.4 Stirrup strain

Strain of stirrup in the shear span of NCB and UCB is presented in Fig. 8. It can be seen that the strain of stirrup in NCB is larger than that in UCB in the same position under the same load, which shows that the stress of stirrup in NCB is larger than that in UCB. The precast UHPC element has excellent tensile properties and shear properties, and it can transfer the shear on diagonal section with stirrup together, so it can decrease the stress in the stirrup.

3.2.5 Connector deformation

In the pure bending section of UCB, the strain gauges in four bolts were attached. Before longitudinal rebar yield, the strain in bolt connector is small, and it is about 150 $\mu\varepsilon$ at longitudinal rebar yielding status. After the longitudinal rebar yield, strain of bolt began to increase. The average strain of the four bolts in different load level is presented in Fig. 9. Therefore, the interface stress at the first stage i.e., prior to cracking load, is low, but increases significantly beyond the cracking stage from the strain variation of the bolt. The bonding between UHPC permanent form and core RC at the first stage is effective, and the connector design is necessary at the interface nonlinear stage.

3.3 Analysis of the result and discussion

3.3.1 Crack distribution

Fig. 5 shows that the stiffness of UCB increases greatly compared to NCB, and the crack morphology in UCB shows parallel micro crack feature, and there are many micro cracks but the width is small, which is quite distinct from NCB. This character can be attributed to the contribution of the constraints of precast UHPC element.

3.3.2 Strength

The cracking load is increased by 112% and ultimate bearing capacity is increased by 5.8% as

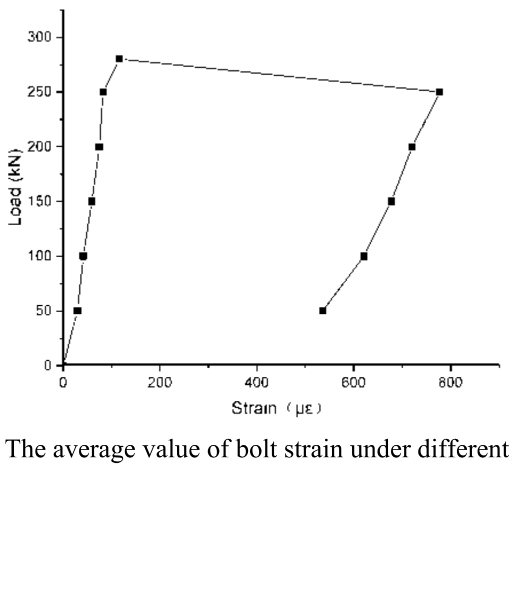

Fig. 9 The average value of bolt strain under different load

shown in Table 3. It can be also attributed to the high tensile strength and high toughness of precast UHPC element, so precast UHPC element increases the cracking load of the whole beam. For UCB, the yielding load is almost equal to the ultimate load and there has no deflection hardening stage. For NCB, the stable final load 276 kN not the peak load is considered as the ultimate load considering the ultimate compression state of compression zone.

3.3.3 Deformation and ductility

The elasticity modulus of UHPC is equal to 45 GPa and it is slightly higher than that of NC 35 GPa, and the U shaped UHPC element makes that the stiffness of UCB is larger than the stiffness of NCB, so the deformation of UCB is smaller than NCB under the same loading conditions.

The mid-span displacement was 0.54 mm when NCB cracked while the mid-span displacement was 0.97 mm when UCB cracked, so mid-span displacement in UCB at the first crack increases by 80%. After longitudinal rebar yield, because normal concrete and UHPC in tension zone do not work again, so the final deformation properties of NCB are close to UCB. The stiffness of the main crack section in mid-span is similar, so displacement increment is also very close.

The interfacial deformation can be analyzed from Fig. 9. In the stage prior to longitudinal rebar yielding, the bolt strain is within 200 $\mu\varepsilon$ which indicates that the interfacial debonding stress is low. However, the interfacial debonding stress increase beyond the yielding state. The effective constructive design between UHPC permanent form and core concrete is necessary.

The initial crack displacement of UCB is increased by 80% compared to NCB. Precast UHPC element has a significant toughening effect, and it is stronger for deformation ability, so the ductility of UCB is better than that of NCB which can be seen from the deflection ductility factor variation. The deflection ductility index is improved from 2.87 to 6.34.

4. Conclusions

- Precast UHPC element has an important influence on crack mode of a bending RC beam. UHPC permanent form changes flexural crack mode of reinforced concrete beam to multiple and fine crack, so UCB has better durability compared to NCB. UHPC can also avoid effectively forming cracks in the normal use stage.
- The first cracking strength and ultimate bearing capacity can be significantly improved by the precast UHPC unit. From the test result, compared to NCB, cracking strength of UCB is increased by about 110%, and the flexural bearing capacity is increased by about 5%. Therefore, the reinforcement ratio can be reduced. The minimum reinforcement ratio and balanced state should be redefined for normally reinforcement steel and concrete according to this composites beam failure mode. The theoretical model will be studied.
- Effects of precast UHPC element on member deformation and ductility are also significant from the deflection ductility factor variation.

Acknowledgments

The authors would like to thank the National Natural Science Foundation of China (51008088) (51678196), China Scholarship Council (CSC), the Fundamental Research Funds for the Central Universities (Grant No. HIT. NSRIF. 2013112), Harbin City Science and Technology Innovation Talents Special Funds (2011RFLXG014), and Heilongjiang Province Natural Science Fund

(E200911) (E2015014) for providing funding to this project, the National Key Technology Research and Development Program of China under Grant No. 2011BAJ10B0102, for the supporting the authors' work described herein.

References

Benjamin, A.G. (2006), "Structural behavior of ultra-high performance concrete prestressed I-girders", *FHWA-HRT-06-115*, *Federal Highway Administration*, New Jersey Ave., SE Washington, USA.

Bencardino, F. (2013), "Mechanical parameters and post-cracking behavior of HPFRC according to three-point and four bending test", *Adv. Civil Eng*., 1-9.

Bencardino, F. and Condello, A. (2014), "Experimental study and numerical investigation of behavior of RC beams strengthened with steel reinforced grout", *Comput. Concrete*, *Int. J*., **14**(6), 711-725.

Guler, S., Copur, A. and Aydogan, M. (2012), "Flexural behaviour of square UHPC-filled hollow steel section beams", *Struct. Eng. Mech*., *Int. J*., **43**(2), 225-237.

Guler, S., Çopur, A. and Aydogan, M. (2013), "Nonlinear finite element modeling of FRP-wrapped UHPC columns", *Comput. Concrete*, *Int. J*., **12**(4), 413-429.

Habel, K. (2004), "Structural behaviour of element combining ultra-high performance fibre reinforced concretes(UHPFRC) and reinforced concrete", Ph.D. Dissertation; Ecol Polytechnique Federal de Lausanne, Lausanne, Switzerland.

Hong, S.G. and Kang, S.H. (2013), "Formwork development using UHPFRC", *Proceedings of the Rilem-fib-AFGC International Symposium on Ultra-High Performance Fibre-Reinforced Concrete*, Marseille, France, October.

Lou, T., Lopes, S.M.R. and Lopes, A.V. (2015), "Redistribution of moments in reinforced high-strength concrete beams with and without confinement", *Struct. Eng. Mech*., *Int. J*., **55**(2), 379-398.

Massicotte, B., Dagenais, M.A. and Lagier, F. (2013a), "Strengthening Bridge Piers using Ultra High Performance Fiber Reinforced Concrete", *Proceeding of the 7th National Seismic Conference on Bridges and Highways*, Oakland, CA, USA, May.

Massicotte, B., Dagenais, M.A. and Lagier, F. (2013b), "Performance of UHPFRC jackets for the seismic strengthening of bridge piers", *Proceedings of the Rilem-fib-AFGC International Symposium on Ultra-High Performance Fibre-Reinforced Concrete*, Marseille, France, October.

Mohanammed, T.J., Abu Bakar, B.H. and Bunnori, N.M. (2015), "Strengthening of reinforced concrete beams subjected to torsion with UHPFC composites", *Struct. Eng. Mech*., *Int. J*., **56**(1), 123-136.

Noshiravani, T. and Bruhwiler, E. (2013), "Experimental investigation on reinforced ultra-high-performance fiber-reinforced concrete composite beams subjected to combined bending and shear", *ACI Struct. J*., **110**(2), 251-261.

Rizzuti, L. and Bencardino, F. (2014), "Effect of fibre volume fraction on the compressive and flexural experimental behavior of SFRC", *Contemporary Eng. Sci*., **7**, 379-390.

Wu, X.G., Han, S.M. and Xu, S.L. (2008), "Pseudo strain hardening model of ultra high performance cementitious composites under flexural loading", *Acta Materiae Compositae Sinica*, **25**(2), 129-134.

Wu, X.G., Zhao, X.Y. and Han, S.M. (2011), "Structural analysis of circular UHPC form for hybrid pier under construction loads", *Steel Compos. Struct*., *Int. J*., **12**(2), 167-180.

Wu, X.G., Yu, Q., Zhao, X.Y., Zheng, W.Z. and Han, S.M. (2013a), "Uniaxial compressive strength of durable hybrid pier with UHPC permanent form", *Proceedings of the Rilem-fib-AFGC International Symposium on Ultra-High Performance Fibre-Reinforced Concrete*, Marseille, France, October.

Wu, X.G., Yang, J. and Mpalla, I.B. (2013b), "Preliminary design and structural responses of typical hybrid wind tower made of ultra high performance cementitious composites", *Struct. Eng. Mech*., *Int. J*., **48**(6), 791-807.

Wu, X.G., Hu, Q., Zou, R.F., Zhao, X.Y. and Yu, Q. (2014), "Structural behaviors of sustainable hybrid columns under compression and flexure", *Struct. Eng. Mech*., *Int. J*., **52**(5), 857-873.

Wirojjanapirom, P., Matsumoto, K. and Niwa, J. (2013), "Experimental Study on Shear Behavior of RC Beams Using U-Shape UFC Permanent Formwork with Shear Keys and Bolts", *J. Japan Soc. Civil Eng., Ser. E2* (*Materials and Concrete Structures*), **69**(1), 67-81.

Yuan, F., Pan, J.L. and Leung, C.K.Y. (2013), "Flexural behaviors of ECC and concrete /ECC composite beams reinforced with basalt fiber reinforced polymer", *J. Compos. Construct.*, **17**(5), 591-602.

Yuan, F., Pan, J.L., Dong L.T. and Leung, C.K.Y. (2014), "Mechanical Behaviors of Steel Reinforced ECC or ECC/Concrete Composite Beams under Reversed Cyclic Loading", *J. Mater. Civil Eng.*, **26**(8), 86-88.

CC